

Bounds for the complex dielectric constant of a two-component composite material

David J. Bergman

Department of Physics and Astronomy, Tel Aviv University, Tel Aviv 69978, Israel

(Received 3 March 1980; revised manuscript received 30 June 1980)

Rigorous bounds are derived for the bulk effective complex dielectric constant K_e of a two-component composite medium in two cases: (a) when only the complex dielectric constants of the two components are known and (b) when, in addition to that, also the volume fractions are known. The bounds have a very simple geometric representation in the complex K_e plane. From these bounds, some useful conclusions are drawn with respect to measured values of these constants in various types of composites.

I. INTRODUCTION

The existence of rigorous bounds on the possible values of the effective bulk dielectric constant ϵ_e of a composite material (i.e., a macroscopically inhomogeneous material) was recognized long ago.¹ Over the years various types of bounds have been found, based on different types of information that is available about the microscopic geometry of the composite. While much of this material is summarized in Beran's book,² I would also draw special attention to the work of Hashin and Shtrikman,³ Prager,⁴ and Bergman.⁵⁻⁷ All of these treatments derived bounds for the case when all of the dielectric constants in the problem were real and positive. Because the problem of calculating the effective bulk electrical conductivity, thermal conductivity, diffusivity, or magnetic permeability is identical mathematically to the problem of finding ϵ_e , these treatments lead of course to similar bounds for all of these quantities. All of these bounds are again confined to the case where all the material constants in the problem are real and positive.

Bounds on the dielectric constant for the case when the components are lossy, i.e., when the dielectric constants are complex, have been derived by Shulgasser and Hashin⁸ who considered a two-component composite of low-loss dielectrics. A more general discussion of bounds of lossy composite dielectrics has been given by Shulgasser in his thesis.⁹ That discussion is based on a variational principle, and the results are in the form of separate bounds on the real and imaginary parts of the complex bulk effective dielectric constant K_e . In this context I should also mention some bounds on the complex material constants of viscoelastic composites, which were derived by Christensen¹⁰ and by Roscoe.¹¹

In this article I derive two sets of exact bounds on K_e for a two-component composite where both components have complex dielectric constants K_1 , K_2 . These bounds which, to the best of my knowledge, have not been known previously, have the

form of a restricted region in the complex plane in which K_e must lie. This means that for each value of $\text{Im } K_e$, one usually obtains a different pair of bounds on $\text{Re } K_e$, and vice versa. Because these bounds are exact, they involve no assumptions about the composite other than that the dielectric properties of each component are fully described by its dielectric constant, and that surface or interface effects (such as tunneling or surface conductivity) are unimportant.

I obtain one set of bounds for the case where K_1 and K_2 are known, but no other information is available about the composite. Another improved set of bounds is obtained for the case when the volume fractions p_1 , p_2 of the two components are also known. I derive explicit expressions for these bounds, and I also show that they have a very simple and beautiful geometrical representation in the complex plane, which enables them to be constructed on graph paper simply by the use of a ruler and compass!

The outline of the rest of this article is as follows: In Sec. II I derive the first set of bounds by using a method similar to Roscoe's method.¹¹ In Sec. III I employ a more advanced method for finding bounds that is due to Bergman.⁷ In this way I rederive the first bounds and also get the improved bounds. Both sets of bounds are obtained in a modified representation of K_e which is especially convenient both for the derivation process and for the representation of the final results. In Sec. IV I discuss possible applications of these bounds as well as extensions and improvements. Consequences that follow from the bounds for some measured properties of composite materials are also discussed.

II. SIMPLE BOUND BY ELEMENTARY METHOD

In this section, I derive rigorous bounds on the bulk complex dielectric constant of a two-component composite material, both components having isotropic electrical properties, when all that is known are the corresponding constants of each

component. The method used is due to Roscoe,¹¹ and it has the advantage of yielding not only the bounds themselves, but also the special microscopic geometries for which these bounds are attained.

The dielectric constant of each component can have an imaginary part at nonzero frequencies either due to dielectric losses, or due to the presence of a nonzero dc conductivity σ . In the latter case, assuming that all electromagnetic fields have a time dependence $e^{-i\omega t}$, we can write the complex dielectric constant in the form

$$K = \epsilon - \frac{4\pi\sigma}{i\omega}. \quad (2.1)$$

Whatever the cause of the complex nature of K , its precise value will vary from point to point, fluctuating between the two allowed values K_1, K_2 . We can make this spatial dependence explicit with the help of the step functions $\Theta_1(\vec{r}), \Theta_2(\vec{r})$:

$$K(\vec{r}) = \sum_{j=1,2} K_j \Theta_j(\vec{r}), \quad (2.2)$$

where $\Theta_j(\vec{r})$ is 1 if \vec{r} is in the volume of component j , and 0 otherwise.

Using a bracket notation to denote volume averages

$$\langle A \rangle \equiv \frac{1}{V} \int A(\vec{r}) d^3r, \quad (2.3)$$

we can define the bulk effective complex dielectric constant of the composite K_e by

$$K_e \langle \vec{E} \rangle \equiv \langle K \vec{E} \rangle, \quad (2.4)$$

where $\vec{E}(\vec{r})$ is the electric field. Using the fact that $\vec{E} = -\nabla\phi$ is the gradient of a scalar potential (this means that the frequency ω must be small enough so that we may use the static limit of Maxwell's equations), we can show that K_e also satisfies the following equation:

$$K_e \langle \vec{E}^* \rangle \cdot \langle \vec{E} \rangle = \langle K \vec{E}^* \cdot \vec{E} \rangle. \quad (2.5)$$

This is shown by successive volume-to-surface and surface-to-volume transformations of the right-hand side of this equation, which change it to the right-hand side of Eq. (2.4) multiplied by $\langle \vec{E}^* \rangle$.

Writing K_j in the form

$$K_j = K'_j + iK''_j, \quad j=1,2, \quad (2.6)$$

where K'_j, K''_j are both real, we now separate Eq. (2.5) into two real equations as

$$K'_e \langle \vec{E}^* \rangle \cdot \langle \vec{E} \rangle = \langle K' \vec{E}^* \cdot \vec{E} \rangle, \quad (2.7)$$

$$K''_e \langle \vec{E}^* \rangle \cdot \langle \vec{E} \rangle = \langle K'' \vec{E}^* \cdot \vec{E} \rangle.$$

We then choose u and v to be solutions of the two

equations

$$uK'_j + vK''_j = 1, \quad j=1,2 \quad (2.8)$$

so that

$$(uK'_e + vK''_e) \langle \vec{E}^* \rangle \cdot \langle \vec{E} \rangle = \langle \vec{E}^* \cdot \vec{E} \rangle. \quad (2.9)$$

Since we must always have

$$\langle \vec{E}^* \rangle \cdot \langle \vec{E} \rangle \leq \langle \vec{E}^* \cdot \vec{E} \rangle, \quad (2.10)$$

we now obtain our first bound

$$uK'_e + vK''_e \geq 1. \quad (2.11)$$

In order to determine for what kind of microgeometry the equality sign holds, we note that equality in Eq. (2.10) will only hold if $\vec{E}(\vec{r})$ is everywhere independent of \vec{r} . From the basic equation $\vec{\nabla} \cdot K \vec{E} = 0$ we now obtain $\vec{E} \cdot \vec{\nabla} K = 0$ for this case. From Eq. (2.2) we see that $\vec{\nabla} K$ is nonzero only at the K_1, K_2 boundary, and that it is always directed perpendicular to that boundary. Thus, for equality to hold in Eq. (2.11) the boundary between the K_1 and K_2 components must everywhere be parallel to the constant direction of \vec{E} . The two components are then arranged in cylinders which are parallel to the field direction.

In order to find the other bound, we consider the complex displacement field

$$\vec{D}(\vec{r}) \equiv K \vec{E}, \quad (2.12)$$

which for a conductor is proportional to the sum of conduction and displacement currents:

$$K \vec{E} = -\frac{4\pi}{i\omega} \left(\sigma - \frac{i\omega\epsilon}{4\pi} \right) \vec{E}. \quad (2.13)$$

In terms of \vec{D} , Eqs. (2.4) and (2.5) become

$$\langle \vec{D} \rangle = \left\langle \frac{\vec{D}}{K} \right\rangle, \quad (2.14)$$

$$K_e \left\langle \frac{\vec{D}}{K} \right\rangle^* \cdot \left\langle \frac{\vec{D}}{K} \right\rangle = \left\langle \frac{\vec{D}^* \cdot \vec{D}}{K^*} \right\rangle.$$

Combining these equations, and taking the complex conjugate, we finally obtain

$$\frac{1}{K_e} \langle \vec{D}^* \rangle \cdot \langle \vec{D} \rangle = \left\langle \frac{D^* \cdot D}{K} \right\rangle. \quad (2.15)$$

As before, this equation can be separated into real and imaginary parts. Choosing u' and v' to be solutions of the equations

$$u' \operatorname{Re} \frac{1}{K_j} - v' \operatorname{Im} \frac{1}{K_j} = 1, \quad j=1,2 \quad (2.16)$$

we now get

$$\left(u' \operatorname{Re} \frac{1}{K_e} - v' \operatorname{Im} \frac{1}{K_e} \right) \langle \vec{D}^* \rangle \cdot \langle \vec{D} \rangle = \langle \vec{D}^* \cdot \vec{D} \rangle. \quad (2.17)$$

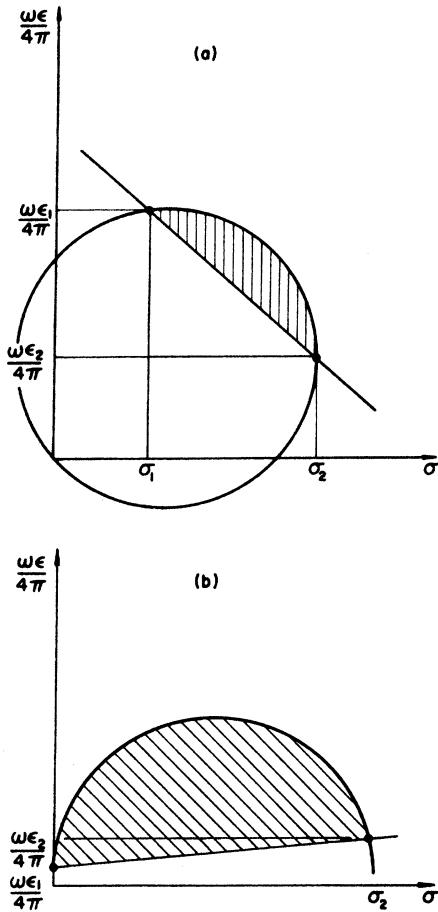


FIG. 1. (a) Graphic representation of bounds in the σ , $\omega\epsilon/4\pi$ plane. The straight line is the bound of equations (2.8) and (2.11). The circle is the bound of equations (2.16) and (2.19). The hatched area is the region where the bulk effective constants must lie. (b) Same as (a) but for the special case when $\sigma_1 = 0$ and $\sigma_2 \gg \omega\epsilon_2/4\pi$ and $\sigma_2 \gg \omega\epsilon_1/4\pi$. It is clear that in this case ϵ_e can be much greater than both ϵ_1 and ϵ_2 .

Noting that

$$\langle \vec{D}^* \rangle \cdot \langle \vec{D} \rangle \leq \langle \vec{D}^* \cdot \vec{D} \rangle, \quad (2.18)$$

we now find our second inequality

$$u' \operatorname{Re} \frac{1}{K_e} - v' \operatorname{Im} \frac{1}{K_e} = \frac{u' K_e + v' K_e''}{(K_e')^2 + (K_e'')^2} \geq 1. \quad (2.19)$$

In order to find the microgeometry that corresponds to the equality sign, we note that $\vec{D}(\vec{r})$ must be independent of position. From the fact that $\vec{\nabla} \times \vec{E} = 0$ (static limit) we now find

$$\vec{\nabla} \times \frac{\vec{D}}{K} = -\vec{D} \times \vec{\nabla} \frac{1}{K} = 0. \quad (2.20)$$

By Eq. (2.2) the vector quantity $\vec{\nabla}(1/K)$ is again nonzero only at the K_1, K_2 boundary, and is always

perpendicular to that boundary. Therefore, equality will hold in Eq. (2.19) only if that boundary is everywhere perpendicular to the constant direction of \vec{D} . This is a microgeometry where the two components are in the form of flat, parallel slabs perpendicular to the field direction.

The bounds described by Eqs. (2.11) and (2.19) have a very simple geometrical interpretation in the complex K plane. This is shown graphically in Fig. 1(a), where we have assumed a purely real ϵ and a purely real σ , and the axes correspond to the real and imaginary parts of the complex conductivity

$$-\frac{i\omega}{4\pi} K = \sigma - \frac{i\omega\epsilon}{4\pi}. \quad (2.21)$$

In such a plot, each component is represented by a point, as is the mixture. The first bound [Eq. (2.11)] means that the mixture point and the origin must lie on opposite sides of the straight line defined by the two component points. The second bound [Eq. (2.19)] requires that the mixture point lie inside the circle passing through the two-component points and the origin. The straight line is reached in the parallel cylinders microgeometry, while the circle is reached in the parallel slab microgeometry.

III. ADVANCED METHOD AND IMPROVED BOUNDS

In this section we will use several different spectral representations for the function $K_e(K_1, K_2)$ as follows:

$$\begin{aligned} s &\equiv \frac{K_2}{K_2 - K_1}, \quad t \equiv \frac{K_1}{K_1 - K_2} = 1 - s, \\ F(s) &\equiv 1 - \frac{K_e}{K_2} = \sum_{\alpha} \frac{B_{\alpha}}{s - s_{\alpha}}, \\ G(t) &\equiv 1 - \frac{K_e}{K_1} = \sum_{\alpha} \frac{A_{\alpha}}{t - t_{\alpha}}, \\ H(t) &\equiv 1 - \frac{K_2}{K_e} = \sum_{\alpha} \frac{C_{\alpha}}{t - \bar{t}_{\alpha}}, \\ E(s) &\equiv 1 - \frac{K_1}{K_e} = \sum_{\alpha} \frac{D_{\alpha}}{s - \bar{s}_{\alpha}}. \end{aligned} \quad (3.1)$$

The poles s_{α} , \bar{s}_{α} , $t_{\alpha} = 1 - s_{\alpha}$, $\bar{t}_{\alpha} = 1 - \bar{s}_{\alpha}$, and the residues A_{α} , B_{α} , C_{α} , D_{α} in these equations are all real, and are between 0 and 1. Moreover, the sum of the residues is equal to one of the volume fractions

$$\begin{aligned} \sum_{\alpha} B_{\alpha} &= \sum_{\alpha} C_{\alpha} = p_1, \\ \sum_{\alpha} A_{\alpha} &= \sum_{\alpha} D_{\alpha} = p_2 = 1 - p_1. \end{aligned} \quad (3.2)$$

The representations of Eq. (3.1) were derived and discussed in Ref. 7. The function $F(s)$ is defined in Eq. (4.2) of Ref. 7, while $H(t)$ is named $\Phi(t)$ and defined in Eq. (4.29) of that reference. Alternatively the properties of $H(t)$ may be found from the properties of $F(s)$ by the following considerations: For $\text{Im}s \neq 0$ we always have $\text{Im}F \neq 0$. Therefore $F(s)=1$ only on the real axis. Furthermore, this can occur only for $0 < s \leq 1$, since for other real values of s (which correspond to the "physical case" $K_1 > 0, K_2 > 0$) $F(s) < 1$ (because then also $K_e > 0$). The zeros of $F(s) - 1$, one of which is found between every two neighboring poles of $F(s)$, are denoted by \bar{s}_α , and they lead to the poles of $H(t)$ at $\bar{t}_\alpha = 1 - \bar{s}_\alpha$. The values of \bar{t}_α are thus all real, and also lie between 0 and 1. The zeros of $F(s)$ are all simple, and the derivative satisfies $F'(\bar{s}_\alpha) < 0$. Hence the residues of $H(t)$ are all real and positive. Expanding the spectral representations of $F(s)$ and $H(t)$ for large s and t we find the following asymptotic expressions for K_e/K_2 :

$$\begin{aligned} \frac{K_e}{K_2} &\cong 1 - \frac{1}{s} \sum_{\alpha} B_{\alpha}, \\ \frac{K_e}{K_2} &\cong 1 + \frac{1}{t} \sum_{\alpha} C_{\alpha}. \end{aligned} \quad (3.3)$$

$$\text{Re} \delta F = \sum_{\alpha} \left(\frac{\delta B_{\alpha} (\sigma - s_{\alpha})}{(\sigma - s_{\alpha})^2 + \rho^2} + \frac{B_{\alpha} \delta s_{\alpha} [(\sigma - s_{\alpha})^2 - \rho^2]}{[(\sigma - s_{\alpha})^2 + \rho^2]^2} \right), \quad (3.5)$$

$$\frac{\text{Im} \delta F}{-\rho} = \sum_{\alpha} \left(\frac{\delta B_{\alpha}}{(\sigma - s_{\alpha})^2 + \rho^2} + \frac{2B_{\alpha} \delta s_{\alpha} (\sigma - s_{\alpha})}{[(\sigma - s_{\alpha})^2 + \rho^2]^2} \right). \quad (3.6)$$

We will now treat $\text{Im}F(s)$ as if it were given, thus constituting a constraint on the possible variations $\delta s_{\alpha}, \delta B_{\alpha}$, when we attempt to maximize or minimize $\text{Re}F(s)$. The constraint is taken into account by using it to express one of the variations, i.e., δB_0 , in terms of the others. This is done by considering an appropriate combination of Eqs. (3.5) and (3.6), namely,

$$\text{Re} \delta F + \frac{\sigma - s_0}{\rho} \text{Im} \delta F = -\frac{B_0 \delta s_0}{(\sigma - s_0)^2 + \rho^2} + \sum_{\alpha \neq 0} \left(\frac{\delta B_{\alpha} (s_0 - s_{\alpha})}{(\sigma - s_{\alpha})^2 + \rho^2} + \frac{B_{\alpha} \delta s_{\alpha} [(\sigma - s_{\alpha})(2s_0 - \sigma - s_{\alpha}) - \rho^2]}{[(\sigma - s_{\alpha})^2 + \rho^2]^2} \right). \quad (3.7)$$

Because the coefficient of δs_0 is negative, we can increase $\text{Re}F$ by taking $\delta s_0 < 0$ until $s_0 = 0$. Since we could have chosen s_0 to be the largest pole, this leads to a single-pole function as an upper bound on $\text{Re}F$, namely,

$$\text{Re} F(s) \leq \text{Re} \left(\frac{B_0}{s} \right) = \frac{\sigma B_0}{\sigma^2 + \rho^2}. \quad (3.8)$$

It still remains to determine B_0 , and this must be done by solving the constraint equation

$$\text{Im} F(s) = -\frac{\rho B_0}{\sigma^2 + \rho^2}. \quad (3.9)$$

Using B_0 as determined by this equation, Eq. (3.8)

From the fact that $t \cong -s$, we finally get $\sum_{\alpha} C_{\alpha} = \sum_{\alpha} B_{\alpha}$, so that the sum rule for $F(s)$ engenders a similar sum rule for $H(t)$, and we also get that $0 < C_{\alpha} < 1$.

The remaining functions, $G(t)$ and $E(s)$, are obtained from $F(s)$ and $H(t)$, respectively, by switching the roles of the two components K_1 and K_2 , and the same is true for their spectral representations and sum rules. We note that the poles and the residues in all of these expansions are determined entirely by the microscopic geometry of the composite. The physical or material properties of the components, i.e., the values of K_1 and K_2 , enter only through the variable s or t . It was shown in Ref. 7 that by treating the positions and residues of the poles as adjustable parameters, rigorous bounds of various types could very easily be derived. We will adopt this method here.

In order to implement it, we need to calculate the first variation of $\text{Re}F$ and of $\text{Im}F$ when s_{α} and B_{α} are changed by small amounts $\delta s_{\alpha}, \delta B_{\alpha}$. Representing the complex variable s by its real and imaginary parts

$$s = \sigma + i\rho, \quad (3.4)$$

we thus get

becomes

$$\text{Re} F + \frac{\sigma}{\rho} \text{Im} F \leq 0. \quad (3.10)$$

Another inequality can be found by repeating the entire discussion beginning with Eq. (3.4) for the function $H(t)$, and noting that

$$t = 1 - s = 1 - \sigma - i\rho. \quad (3.11)$$

In this way we obtain an inequality analogous to Eq. (3.10), namely

$$\text{Re} H + \frac{1 - \sigma}{-\rho} \text{Im} H \leq 0. \quad (3.12)$$

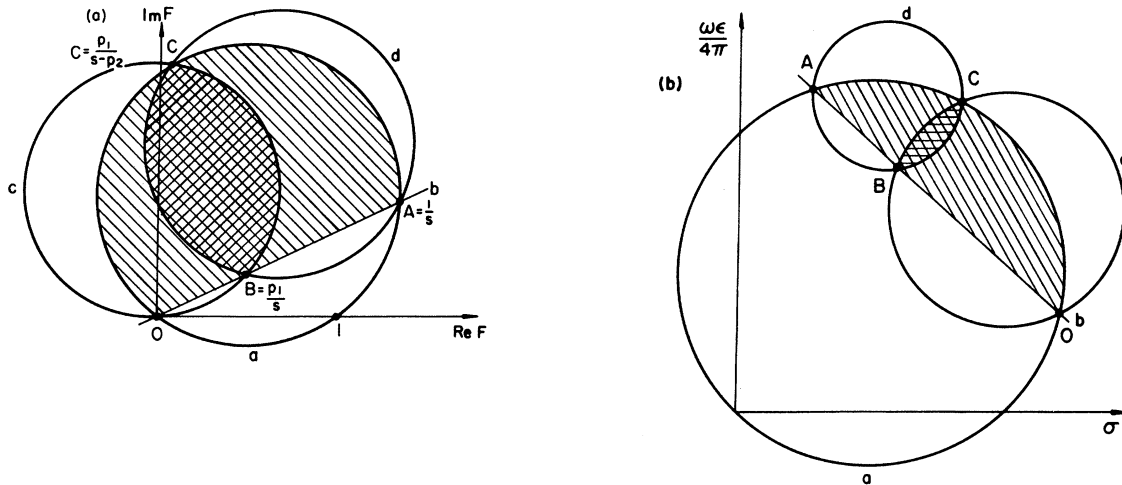


FIG. 2. (a) Drawing of the various bounds derived in this article in the complex F plane. The hatched area between the circle a and the straight line b denotes the bounds obtained only from knowledge of s . The cross-hatched area enclosed by both the circles c and d denotes the bounds obtained when p_1 is also known. Note the special points O , A , B , and C that are marked on the graph which enable all the lines to be constructed geometrically (by a ruler and compass, if desired). (b) Analogous drawing of the same bound in the σ , $\omega\epsilon/4\pi$ plane. Again, the marked special points allow the bounds to be constructed geometrically. In these coordinates, the expressions for the points are more complicated; so we give them here as follows:

$$O = \left(\sigma_2, \frac{\omega\epsilon_2}{4\pi} \right),$$

$$A = \left(\sigma_1, \frac{\omega\epsilon_1}{4\pi} \right),$$

$$B = \left(p_1\sigma_1 + p_2\sigma_2, \frac{\omega}{4\pi} (p_1\epsilon_1 + p_2\epsilon_2) \right),$$

$$C = \left(\left[\sigma_1\sigma_2 - \left(\frac{\omega}{4\pi} \right)^2 \epsilon_1\epsilon_2 \right] (p_1\sigma_2 + p_2\sigma_1) + \left(\frac{\omega}{4\pi} \right)^2 (\sigma_1\epsilon_2 + \epsilon_1\sigma_2)(p_1\epsilon_2 + p_2\epsilon_1), \frac{\omega}{4\pi} \left\{ (\sigma_1\epsilon_2 + \epsilon_1\sigma_2)(p_1\sigma_1 + p_2\sigma_1) - \left[\sigma_1\sigma_2 - \left(\frac{\omega}{4\pi} \right)^2 \epsilon_1\epsilon_2 \right] (p_1\epsilon_2 + p_2\epsilon_1) \right\} \right) \\ \times \left[(p_1\sigma_2 + p_2\sigma_1)^2 + \left(\frac{\omega}{4\pi} \right)^2 (p_1\epsilon_2 + p_2\epsilon_1)^2 \right]^{-1}.$$

Noting also that

$$H(t) = \frac{F(s)}{F(s) - 1}, \quad (3.13)$$

we immediately obtain from this the following inequality for $F(s)$:

$$|F|^2 - \operatorname{Re} F + \frac{1 - \sigma}{\rho} \operatorname{Im} F \leq 0, \quad (3.14a)$$

which can also be written in the form

$$\left| F(s) - \frac{1}{2} - \frac{i(\sigma - 1)}{2\rho} \right|^2 \leq \frac{1}{4} + \left(\frac{\sigma - 1}{2\rho} \right)^2. \quad (3.14b)$$

The inequality of Eq. (3.10) restricts $F(s)$ to lie on one side of a straight line through the origin, while Eq. (3.14b) restricts $F(s)$ to lie inside a circle that also passes through the origin. In Fig. 2(a) we show these two lines, as well as some

points which are sufficient to determine them:

The straight line passes through the origin and also through the point $F = 1/s$. The circle passes through the origin, and through the points $F = 1/s$ and $F = 1$.

These bounds are identical to the ones found in the preceding section. To see this we must transform back to the coordinates used in Fig. 1. This is done by substituting

$$F(s) = 1 - \frac{K_\theta}{K_2} = \frac{\sigma_2 - \frac{i\omega\epsilon_2}{4\pi} - \left(\sigma_\theta - \frac{i\omega\epsilon_\theta}{4\pi} \right)}{\sigma_2 - \frac{i\omega\epsilon_2}{4\pi}} \quad (3.15)$$

in Eqs. (3.10) and (3.14).

The method used above to rederive the results of Sec. II will now be extended to include more information about the composite, namely, the volume fraction p_1 . Because of Eq. (3.2), this means that another constraint is now present on the elementary variations δs_α , δB_α , etc. We use this

constraint to eliminate one more of these elementary variations. We can start from equation (4.10) of Ref. 7, where the constraint $\sum_{\alpha} B_{\alpha} = p_1$ has been used to eliminate δB_0 from the expres-

sion for δF , and proceed to eliminate δs_0 by taking an appropriate combination of $\text{Re } \delta F$ and $\text{Im } \delta F$. In this way we get, after some algebraic manipulations, the following result:

$$\begin{aligned} \text{Re } \delta F + \frac{(\sigma - s_0)^2 - \rho^2}{2\rho(\sigma - s_0)} \text{Im } F = & - \sum_{\alpha \neq 0} \frac{\delta B_{\alpha} (s - s_{\alpha})^2 [\rho^2 + (\sigma - s_0)^2]}{[(\sigma - s_{\alpha})(\sigma - s_0) - \rho^2]^2 + \rho^2 (2\sigma - s_{\alpha} - s_0)^2} \frac{1}{2(\sigma - s_0)} \\ & + \sum_{\alpha \neq 0} \frac{B_{\alpha} \delta s_{\alpha} [\rho^2 + (\sigma - s_{\alpha})(\sigma - s_0)] (s_0 - s_{\alpha})}{[(\sigma - s_{\alpha})^2 + \rho^2]^2} \frac{1}{\sigma - s_0}. \end{aligned} \quad (3.16)$$

Taking s_0 to be the largest pole, and assuming $\sigma > s_0$, we can increase $\text{Re } F$ by taking $\delta B_{\alpha} < 0$ for all $\alpha \neq 0$. In this way an upper bound on $\text{Re } F$ is found in the form of a single-pole function as

$$\text{Re } F \leq \text{Re} \left(\frac{B_0}{s - s_0} \right) = \frac{B_0(\sigma - s_0)}{(\sigma - s_0)^2 + \rho^2}. \quad (3.17)$$

The values of B_0 and s_0 are determined by the two constraints

$$p_1 = B_0, \quad (3.18)$$

$$\text{Im } F = - \frac{B_0 \rho}{(\sigma - s_0)^2 + \rho^2}.$$

This leads to a quadratic equation for s_0 whose solution, recalling the assumption $\sigma > s_0$, is

$$\sigma - s_0 = \left(- \frac{p_1 \rho}{\text{Im } F} - \rho^2 \right)^{1/2}. \quad (3.19)$$

From the assumption $\sigma > s_0$, it also follows that $\text{Re } F > 0$. We can now rewrite Eq. (3.17) as follows:

$$(\text{Re } F)^2 \leq \left(\frac{\sigma - s_0}{\rho} \text{Im } F \right)^2 = -(\text{Im } F)^2 - \frac{p_1}{\rho} \text{Im } F, \quad (3.20a)$$

or, alternatively

$$\left| F(s) + \frac{ip_1}{2\rho} \right|^2 \leq \left(\frac{p_1}{2\rho} \right)^2. \quad (3.20b)$$

$$(\rho^2 + \sigma^2) |F|^2 + (p_2 - 2\sigma) \text{Re } F + (1/\rho)[(2 - p_2)\rho^2 - p_2\sigma^2 + p_2\sigma] \text{Im } F + p_1 \leq 0. \quad (3.24)$$

Again, this inequality is obtained under a certain assumption about σ , namely, $1 - \sigma > t_0$, where t_0 is the largest pole of $G(t)$. By considering the function $E(s)$, the same inequality can be derived for the case when that assumption cannot be satisfied, so that Eq. (3.24) is always valid.

Equations (3.20) and (3.24) restrict $F(s)$ to lie inside two circles. These circles are best characterized by noting some points that they pass through. The circle of Eq. (3.20) passes through

Sometimes it may be impossible to satisfy the assumption $\sigma > s_0$, e.g., when $\sigma \leq 0$. In that case, we repeat the procedure that began with Eq. (3.16) for the function $H(t)$. We will now have to assume $1 - \sigma > t_0 = 1 - s'_0$ or $\sigma < s'_0$, where s'_0 is the smallest value of s for which $F(s) = 1$. In this way we will get the following inequality

$$\left| H(t) - \frac{ip_1}{2\rho} \right|^2 \leq \left(\frac{p_1}{2\rho} \right)^2. \quad (3.21)$$

Using Eq. (3.13), we immediately regain Eq. (3.20), which is thus shown to be valid without any restriction on σ .

Another inequality is obtained by applying the above procedure to the function $G(t)$. In that case we obtain

$$\left| G(t) - \frac{ip_2}{2\rho} \right|^2 \leq \left(\frac{p_2}{2\rho} \right)^2, \quad (3.22)$$

where p_2 now appears in place of p_1 that appeared in previous inequalities. This is due to the fact that the two components have now switched roles. If we substitute the following relation

$$G(t) = \frac{1 - sF(s)}{1 - s} \quad (3.23)$$

into Eq. (3.22) we find, after some manipulations, the following inequality for $F(s)$:

the origin, through the point $F = p_1/s$, which also lies on the straight line of Eq. (3.10), and through the point $F = p_1/(s - p_2)$, which also lies on the circle of Eq. (3.14). These two points correspond to the case of a composite in the form of parallel cylinders and parallel plates, respectively, for which the boundary values of F are realized as we pointed out in Sec. II. The circle of Eq. (3.20) can also be characterized by noting that its center is at $-ip_1/2\rho$, and that it passes through the

origin. The circle of Eq. (3.24) also passes through the two points $F = p_1/s$, $F = p_1/(s - p_2)$, and through the point $1/s$ as well. All three circles, as well as the straight line, are drawn in Fig. 2(a) which shows clearly the region where $F(s)$ is restricted to lie both when p_1 is known and when it is not known.

In order to describe the new bounds in the coordinates σ_g , $\omega\epsilon_g/4\pi$ of Sec. II, we must again use Eq. (3.15). That transformation is a uniform dilation plus a shift of origin, so that circles and straight lines are transformed into similar objects. This leads to a very simple geometric method of constructing the new bounds with the help of a ruler and compass which is explained in Fig. 2(b). Note also that the four points OABC that determine the bounds have a much simpler form in Fig. 2(a) than they do in Fig. 2(b). This simplification is one of the benefits of working with the representation of Eq. (3.1) instead of with the usual complex dielectric constants.

IV. DISCUSSION, CONCLUSIONS, AND APPLICATIONS

We have obtained bounds on the values of the complex bulk dielectric constant of a two-component composite material in the form of rigorously defined regions of the complex plane where these values must lie. The bounds depend on the information that is available. Bounds are obtained even when only the complex dielectric constants of the two components are known, but nothing is known about the microscopic geometry or structure. A knowledge of the volume fraction already results in much better bounds.

To obtain these bounds I used a new approach to the problem of dielectric properties of composites that is based on a recently achieved detailed understanding of the general analytical properties of K_g/K_2 as a function of K_1/K_2 .⁷ Although the bounds of Sec. II were first derived by using a simple variational principle, the more powerful methods of Ref. 7 were essential in leading to the improved bounds of Sec. II. Hopefully these methods will

also enable us to derive yet better bounds when more information is available about the composite.

Some important practical or experimental conclusions can immediately be obtained from the bounds I have found:

(a) From the simple bounds of Sec. II (see Fig. 1) it is clear that, when all the component constants are positive, any effective bulk constant (i.e., either σ_g or ϵ_g) is always greater than the smaller of the two individual component constants

$$\sigma_g \geq \min_{j=1,2}(\sigma_j),$$

$$\epsilon_g \geq \min_{j=1,2}(\epsilon_j).$$
(4.1)

(b) The upper bound on σ_g or ϵ_g is however not so simple. Clearly either one or both of these constants can be greater than $\max(\sigma_j)$ or $\max(\epsilon_j)$, respectively. For example, in Fig. 1(b) we have taken the special case

$$\sigma_1 = 0, \quad \omega\epsilon_i/4\pi \ll \sigma_2 \quad \text{for } i = 1, 2$$
(4.2)

which appropriately describes the situation in sedimentary rocks saturated with brine. The rock component is then a good insulator, while the brine component is a rather good conductor. At frequencies below about 1 MHz the assumptions of Eq. (4.2) are satisfied. It is evident from the graphical representation of the bounds that we can sometimes expect to observe values of ϵ_g that are far greater than either ϵ_1 or ϵ_2 . Such observations have in fact been reported.¹²

(c) When the volume fractions are known, the bounds which are obtained can sometimes be a considerable improvement over the previous bounds [see Fig. 2(b)]. These bounds may be turned around so that when ϵ_g and σ_g are known, they yield a bound for the volume fraction p_1 .

ACKNOWLEDGMENT

I would like to acknowledge useful conversations with Philippe Lacour-Gayet, Pabitra Sen, and Zvi Hashin.

¹O. Wiener, *Abh. Math. Phys. Kl. Saechs. Akad. Wiss. Leipzig* **32**, 509 (1912).

²M. J. Beran, *Statistical Continuum Theories* (Interscience, New York, 1968), Chap. 5.

³Z. Hashin and S. Shtrikman, *J. Appl. Phys.* **33**, 3125-3131 (1962).

⁴S. Prager, *J. Chem. Phys.* **50**, 4305-4312 (1969).

⁵D. J. Bergman, *Phys. Rev. B* **14**, 1531 (1976).

⁶D. J. Bergman, *Phys. Rev. B* **14**, 4304 (1976).

⁷D. J. Bergman, *Phys. Rep.* **43**, 378-407 (1978). [Also published in the *W. E. Lamb Festschrift*, edited by D. Ter-Haar and M. Scully (North-Holland, Amsterdam, 1978), Chap. 9.] See also *Proceedings of the First Conference on the Electrical Transport and Optical Properties of Inhomogeneous Media, Ohio State University, 1977*, edited by J. C. Garland and D. B. Tanner (AIP, New York, 1978), p. 44.

⁸K. Shulgasser and Z. Hashin, *J. Appl. Phys.* **47**, 424-

- 427 (1976).
- ⁹K. Shulgasser, Ph.D. thesis, The University of Pennsylvania, 1967 University Microfilms (unpublished).
- ¹⁰R. M. Christensen, J. Mech. Phys. Solids 17, 23 (1969).
- ¹¹R. Roscoe, J. Mech. Phys. Solids 20, 91-99 (1972).
- ¹²J. Poley, J. Nooteboom, and P. de Waals, Log Anal. 19, 8 (1978).